Mon. Not. R. Astron. Soc. **332,** 529–535 (2002)

The clustering of galaxies around quasars

Guinevere Kauffmann[1]★ and Martin G. Haehnelt[2]
[1]*Max-Planck Institut für Astrophysik, D-85740 Garching, Germany*
[2]*Astrophysics Group, Imperial College of Science, Technology and Medicine, Prince Consort Road, London SW7 2BW*

Accepted 2001 December 11. Received 2001 August 22

ABSTRACT

We study the cross-correlation between quasars and galaxies by embedding models for the formation and evolution of the two populations in cosmological *N*-body simulations. We adopt the quasar evolution model of Kauffmann & Haehnelt, in which supermassive black holes are formed and fuelled during major mergers. We define the 'bias' parameter b_{QG} as the ratio of the cross-correlation function ξ_{QG} to the galaxy autocorrelation function ξ_{GG}. On scales larger than $1\,h^{-1}$ Mpc, the values of b_{QG} predicted by our models at low redshift depend very little on galaxy selection. They measure the characteristic mass of the dark matter haloes that host quasars and can be used to estimate the typical quasar lifetime. In current redshift surveys, such measurements will constrain the lifetimes of low-redshift quasars more accurately than measurements of the quasar autocorrelation function, because galaxies have much higher space densities than quasars. On scales smaller than $1\,h^{-1}$ Mpc, the main contribution to ξ_{QG} comes from quasar/galaxy pairs in the same dark matter halo. The amplitude of ξ_{QG} depends both on the location of the host galaxy and on the density profile of other galaxies within the halo. As a result, measurements on these scales yield information about the processes responsible for fuelling supermassive black holes. At high redshifts our models predict that quasars of fixed luminosity are located in less massive haloes than at low redshift. They are therefore less biased relative to galaxies of given luminosity or stellar mass. We have used the simulations to calculate the evolution of the quasar autocorrelation function. We find that models with quasar lifetimes in the range 10^6–10^7 yr provide a good match to the results of the 2dF QSO survey.

Key words: black hole physics – galaxies: formation – galaxies: nuclei – quasars: general.

1 INTRODUCTION

It has been known for more than three decades that quasars are associated with enhancements in the distribution of galaxies (Bahcall, Schmidt & Gunn 1969). Calculations of the QSO/galaxy correlation functions on small scales (<1 Mpc) have shown that at redshifts $z < 0.4$, quasars typically reside in small to moderate groups of galaxies and not in rich clusters (e.g. Hartwick & Schade 1990; Bahcall & Chokshi 1991; Fisher et al. 1996).

It is considerably more uncertain whether the environments of quasars depend on their optical or radio luminosities, or on redshift. Early studies claimed that radio-loud quasars were located in richer environments than radio-quiet quasars (e.g. Yee & Green 1984, 1987; Ellingson, Green & Yee 1991), but these findings have been contested in a number of recent papers (e.g. Fisher et al. 1996; McLure & Dunlop 2001; Wold et al. 2001). Most studies have not found any relation between the optical luminosity of a quasar and its clustering (Brown, Boyle & Webster 2001; Finn, Impey & Hooper 2001), but there have been a number of papers claiming the existence of a correlation between radio luminosity and environment (e.g. Wold et al. 2001; Finn et al. 2001). The studies of Yee & Green (1987) and Ellingson, Green & Yee (1991) found that high-redshift, radio-loud quasars were located in richer environments than low-redshift, radio-loud quasars, but more recent analyses (e.g. Wold et al. 2001) fail to find any trend with redshift.

Part of the reason for the discrepancies between different studies may be that the quasar samples studied so far are small (typically 20–70 objects) and are selected in widely varying different ways. This situation will soon improve with the availability of a new generation of very large quasar surveys. The 2dF QSO redshift survey (Croom et al. 2001a) will measure redshifts for ~25 000 optically selected quasars with $b_j < 20.85$ and $z < 3$. The Sloan Digital Sky Survey (York et al. 2000) aims to study ~100 000 quasars brighter than $g' \sim 19.7$. The evolution of the redshift-space correlation function of quasars in the 2dF survey has been measured by Croom et al. (2001b). Their study shows that the clustering of quasars in the survey is very comparable to that of L_*

★E-mail: gamk@mpa-garching.mpg.de

© 2002 RAS

galaxies at low redshift, and that the correlation length R_0 remains approximately constant out to $z \sim 2$.

In order to interpret observational results on the clustering properties of quasars, a physical model for the evolution of the quasar population in a cosmological context is required (Haehnelt & Rees 1993). Recently, we (Kauffmann & Haehnelt 2000, hereafter KH; Haehnelt & Kauffmann 2000) introduced a 'unified' model for the evolution of galaxies and quasars in a cold dark matter (CDM) dominated Universe. We assumed that supermassive black holes were formed and fuelled during major mergers. If two galaxies of comparable mass merged, their central black holes coalesced and a few percent of the gas in the merger remnant was accreted by the new black hole over a time-scale of a few times 10^7 yr. KH showed that their model could reproduce quantitatively the observed relation between bulge velocity dispersion and black hole mass in nearby galaxies, the strong evolution of the quasar population with redshift and the observed relation between the luminosities of quasars and their host galaxies.

In this paper, we extend the model of KH to study the galaxy environments and the clustering properties of quasars as a function of optical luminosity and of redshift. To do this, we combine the KH quasar evolution model with a set of cosmological *N*-body simulations in which galaxy formation is included using simple recipes from standard semi-analytic models (Kauffmann et al. 1999a). This provides a fully spatially resolved simulation of the clustering of both galaxies and quasars at a series of redshifts. In Section 2, we briefly review the techniques used for following quasar evolution in *N*-body simulations and we discuss the relation between quasars and dark matter haloes in the simulation. In Section 3, we calculate the clustering of galaxies around quasars at low redshift. In Section 4, we predict how quasar/galaxy correlations should evolve to high redshift. In Section 5, we calculate the evolution of the quasar autocorrelation function and in Section 6, we summarize our results.

2 INCLUDING QUASARS AND GALAXIES IN COSMOLOGICAL *N*-BODY SIMULATIONS

The techniques used to include galaxy formation in cosmological *N*-body simulations are described in detail in Kauffmann et al. (1999a). This paper also describes the global properties of galaxies at $z = 0$ in the simulation, including the luminosity function and the two-point correlation function. The evolution of galaxy clustering to high redshift is discussed in Kauffmann et al. (1999b).

Briefly, a friends-of-friends group-finding algorithm is used to identify virialized dark matter haloes in the simulation at a series of closely spaced redshifts from $z \sim 20$ to the present. A halo merging tree is constructed, which links haloes at $z = 0$ to their progenitors at each earlier output time. The galaxy formed from gas cooling in a dark matter halo is assigned the index of the most bound particle in that halo and is referred to as the 'central galaxy' of that halo. The galaxy remains identified with the same particle when its halo is accreted by a larger group or cluster and it becomes a 'satellite'. A satellite can merge with the central galaxy on a dynamical friction time-scale. If the ratio of the masses of the merging satellite and the central galaxy is greater than 0.3, we call this a 'major merger' and an elliptical merger remnant is formed. Following KH, a fraction $f_{\rm BH}$ of the available gas is accreted by the black hole and the remainder will be converted into stars over a short (10^8 yr) time-scale in a 'burst'. Note that in our scheme, the quasar is always located at the position of the central galaxy of the halo. In Section 3, we will explore what happens if we relax this assumption.

In this paper, we study a ΛCDM model with $\Omega = 0.3$, $\Lambda = 0.7$, $\sigma_8 = 0.9$ and $H_0 = 70\,{\rm km\,s^{-1}\,Mpc^{-1}}$. The simulation (one of the two analysed in Kauffmann et al. 1999a) contains 17 million particles of mass $2 \times 10^{10}\,{\rm M_\odot}$ in a periodic box of $L = 141\,h^{-1}$ Mpc. We will restrict our analysis to quasars that form in haloes more massive than $2 \times 10^{12}\,{\rm M_\odot}$ (i.e. containing at least 100 particles), for which the simulation is able to provide a rough merging history.

We have checked that when we parametrize the fraction of gas accreted by a black hole during a merger in the same way as in our previous work using analytic merger trees, we obtain a relation between black hole mass and bulge velocity dispersion with the same zero point. The relation derived from the simulations exhibits considerably more scatter, because the merging histories of haloes are not followed as accurately in the simulation. Merger trees derived using analytic methods (e.g. Kauffmann & White 1993) are not limited by mass resolution, but have the disadvantage that these are not able to specify the positions of haloes and how they evolve with time. If we restrict our analysis to haloes containing at least a thousand particles, we obtain a tighter relation that is in much better agreement with the analytic models, but we are then only able to follow the evolution of very bright quasars and there are not many such objects in the simulation, particularly at high redshifts. We have adopted the 100 particle limit as a compromise, and we caution that higher resolution simulations are needed to address the scatter around the mean relations that we present in this paper. We also focus on the clustering properties of quasars at $z < 2$, where there are still plenty of haloes more massive than 100 particles in the simulations. Simulations of larger volumes at the same resolution are required in order to extend our analysis to redshifts beyond 2.

The KH model assumes that quasar activity is triggered by major merging events. In practice, a variety of different physical mechanisms, including the accretion of small gas-rich satellites, tidal interactions between galaxies, and the accretion of gas in cooling flows, may also result in quasar activity. Recent observations (McLure et al. 1999) suggest that at low redshifts, very luminous quasars with *R*-band magnitudes brighter than −24 are found almost exclusively in elliptical host galaxies, but that fainter quasars are found in spiral as well as elliptical hosts. This suggests that the KH model is appropriate for luminous quasars, but not for Seyferts and other low-level AGN. At high redshifts, much less is known about the properties of quasars and their host galaxies, but it is likely that there are a variety of fuelling mechanisms.

In order to predict the optical luminosities of the quasar, KH assumed a relation between the mass of gas accreted by the black hole $M_{\rm acc}$ and the absolute *B*-band magnitude of the quasar at the peak of its light curve

$$M_B({\rm peak}) = -2.5\log(\epsilon_B M_{\rm acc}/t_q) - 27.45, \quad (1)$$

where ϵ_B is a radiative efficiency constant and t_q is the quasar lifetime. They also assumed that the luminosity of the quasar declined exponentially after the merging event as

$$L_B(t) = L_B({\rm peak})\exp(-t/t_q). \quad (2)$$

KH considered a range of values of t_q and concluded that a value $\sim 10^7$ years provided the best fit to the shape of the observed quasar luminosity function.

In Fig. 1, we plot the mass distributions of dark matter haloes

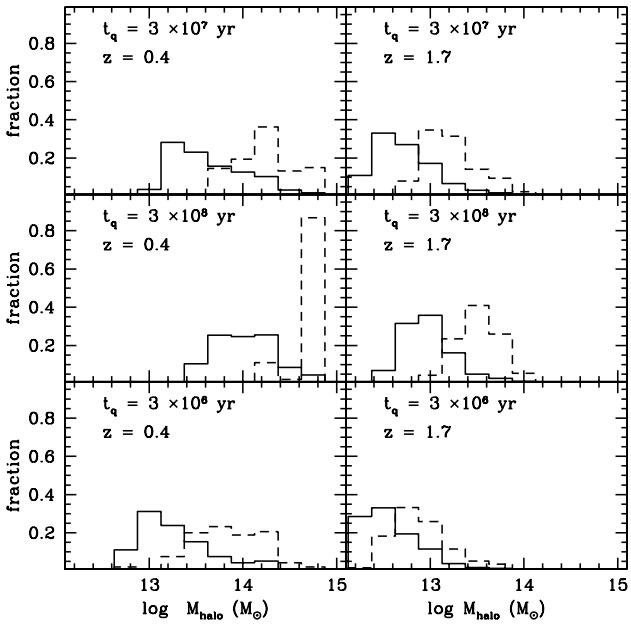

Figure 1. The mass distribution of dark matter haloes that contain quasars with absolute B-band magnitude -23.5 (solid lines) and -25 (dashed lines) for three different values of t_q at $z = 0.4$ and $z = 1.7$.

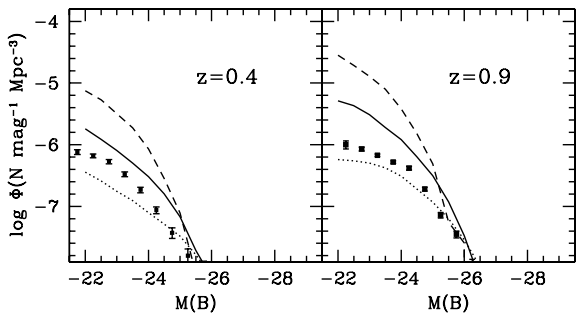

Figure 2. The quasar luminosity function at $z = 0.4$ and $z = 0.9$. The different lines are for different values of the quasar lifetime, t_q: 3×10^7 yr (solid), 3×10^6 yr (dotted) and 3×10^8 yr (dashed). The solid symbols show results from the 2dF 10k catalogue for a cosmology with $\Omega = 0.3$ and $\Lambda = 0.7$ (Croom et al. 2001a).

that host quasars with absolute B-band magnitudes of -23.5 (solid lines) and -25 (dashed lines) for three different choices of the quasar lifetime t_q. Results are shown at $z = 0.4$ and at $z = 1.7$. Note that here and in the rest of this paper, the value of the quasar lifetime t_q is always quoted at $z = 0$. KH assumed that t_q scaled with the host galaxy dynamical time, i.e. $\propto[0.7 + 0.3(1+z)^3]^{-1/2}$ in a ΛCDM cosmology. This means that t_q is a factor of two smaller at $z = 1$ and a factor of three smaller at $z = 2$.

The mass distribution of the host haloes is very sensitive to t_q. Large values of t_q mean that a given mass of accreted gas will have a lower peak luminosity (equation 1). As a result, bright quasars occupy massive haloes, which contain galaxies with large gas masses. In the KH model, where a fixed fraction of the available gas is accreted by the black hole during each merging event and where the peak quasar luminosity scales with the mass of the halo, long quasar lifetimes result in a very steep quasar luminosity function, because quasars sample the exponentially declining high-mass end of the halo mass function. Small values of t_q place quasars in less massive haloes, where the halo mass function is

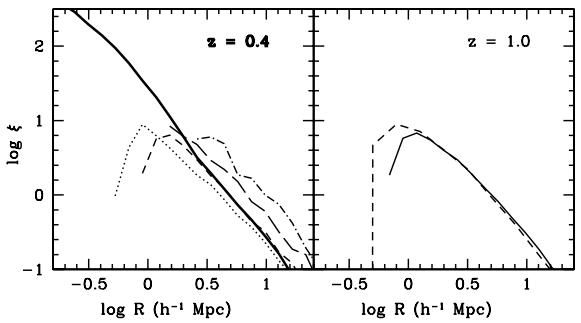

Figure 3. Left: the thick solid line shows the correlation function of the dark matter at $z = 0.4$. The thin lines show the halo correlation functions for haloes in the mass range $10^{12}-3\times10^{12}\,M_\odot$ (dotted), $3\times10^{12}-10^{13}\,M_\odot$ (short-dashed), $10^{13}-3\times10^{13}\,M_\odot$ (long-dashed) and $3\times10^{13}-10^{14}\,M_\odot$ (dot–dashed). Right: the solid line shows the halo autocorrelation function for haloes more massive than $2\times10^{12}\,M_\odot$ in the simulation. The dashed line shows the result obtained when haloes containing quasars are cross-correlated with the full sample.

comparatively flat. As a result, the luminosity function has a much shallower dependence on magnitude. However, as discussed by Haehnelt, Natarajan & Rees (1998), a more complicated fuelling prescription would lead to different inferred lifetimes.

Fig. 2 compares the quasar luminosity functions obtained for three different values of t_q with new data from the 2dF Quasar survey. We plot the luminosity function derived from the 10k catalogue (Croom et al. 2001a) for a cosmology with $\Omega = 0.3$ and $\Lambda = 0.7$. We find that values of t_q in the range 10^6-10^7 yr appear to provide the best fit to the data. Note however, that the differences between the models are largest close to the magnitude limit of the survey, where the data is most subject to photometric incompleteness (Boyle et al. 2000). It is thus difficult to assess whether the apparent 'turnover' in the luminosity function at $M_B > -23$ in the $z = 0.4$ luminosity function and at $M_B > -24$ in the $z = 0.9$ function is real or is caused by selection effects. In the next section, we show that the clustering amplitude of galaxies around bright quasars also constrains the value of t_q in our models. Unlike the luminosity function, the clustering amplitude measures the mass distribution of the dark matter haloes that host quasars of given luminosity, so the derived lifetimes do not depend on the adopted fuelling prescription.

3 QUASAR/GALAXY CORRELATIONS AT LOW REDSHIFT

Analyses of N-body simulations demonstrate that the correlation function of dark matter haloes is proportional to that of the mass over a wide range in scale. For massive haloes, the constant of proportionality is well predicted by a simple analytic model based on an extension of the Press–Schechter theory (Mo & White 1996). More recently, Sheth, Mo & Tormen (2001) have shown that an improved model, based on the assumption that haloes form in an ellipsoidal rather than a spherical collapse, can explain the clustering properties of low mass haloes. In general, more massive haloes are clustered more strongly than less massive haloes. For CDM models, the dependence of clustering on halo mass is weak for haloes with masses below $\sim10^{13}\,M_\odot$, but stronger for more massive haloes (Jing 1998). This is illustrated in the left-hand panel of Fig. 3, where we plot the correlation function of haloes in different mass ranges in our simulation at $z = 0.4$. At this redshift, haloes less massive than a few times $10^{13}\,M_\odot$ are clustered more

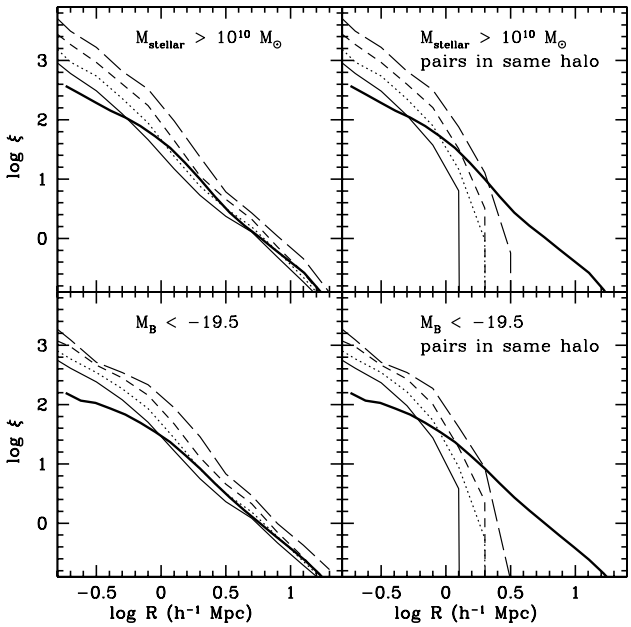

Figure 4. Left: thin lines show quasar/galaxy cross-correlation functions for quasars with *B*-band absolute magnitude of −22.5 (solid), −23.5 (dotted), −24.5 (short-dashed) and −25.5 (long-dashed). The thick solid line shows the galaxy autocorrelation function. Right: thin lines show quasar/galaxy cross-correlation functions for quasar/galaxy pairs in the same dark matter halo. All results are for our fiducial model with $t_q = 3 \times 10^7$ yr at a redshift $z = 0.4$.

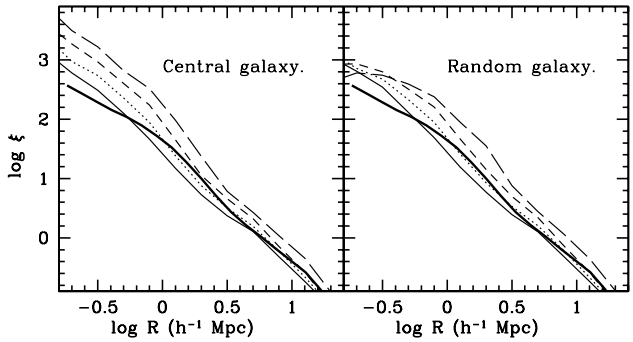

Figure 5. Left: quasar/galaxy cross-correlations for quasars located at the centres of dark matter haloes. Lines are as in Fig. 4. Right: quasar/galaxy cross-correlations for quasars located at the positions of random galaxies in the halo. Results are for our fiducial model with $t_q = 3 \times 10^7$ yr at a redshift $z = 0.4$.

weakly than the underlying dark matter, and haloes more massive than this are clustered more strongly than the dark matter.

In the KH model, quasar activity occurs only in haloes in which the central galaxy has experienced a recent major merger. One might ask whether these haloes are clustered any differently from the average halo of the same mass. The right-hand panel of Fig. 3 compares the autocorrelation function of all haloes more massive than $2 \times 10^{12}\,M_\odot$ with the result obtained when haloes containing quasars are cross-correlated with this sample. Results are shown at $z = 1$, but the conclusion is the same at all redshifts. The clustering of quasar host haloes is indistinguishable from that of ordinary haloes of the same mass, except on scales less than $\sim 1\,h^{-1}$ Mpc, where they are clustered somewhat more strongly. Note that the correlation function falls off steeply on scales smaller than $1\,h^{-1}$ Mpc, because this corresponds roughly to the virial radius of the typical halo in our sample.

The left hand panels of Fig. 4 show quasar/galaxy cross-correlation functions ξ_{QG} for our 'fiducial' model with $t_q = 3 \times 10^7$ yr. The thin lines on the diagram illustrate the results obtained for quasars of different luminosities, and the thick solid line shows the galaxy autocorrelation function for comparison. We select galaxies from the simulation in two different ways: by stellar mass and by *B*-band absolute magnitude. We find that the selection procedure strongly influences the amplitude of the correlation functions on small scales. Galaxies selected by stellar mass are more strongly clustered on scales less than $1\,h^{-1}$ Mpc than galaxies selected by *B*-band absolute magnitude. The right hand panels of Fig. 4 indicate the contribution to ξ_{QG} from quasar/galaxy pairs in the *same dark matter halo*. As can be seen, the contribution to ξ_{QG} from quasars and galaxies in the same halo dominates on scales smaller than $\sim 1\,h^{-1}$ Mpc. The amplitude and slope of ξ_{QG} depend on the density profile of galaxies within individual dark matter haloes. We note that the galaxy density profiles of clusters in our simulation have been compared with observational data and have been found to be in good agreement (Diaferio et al. 2001; Springel et al. 2001).

We have assumed that the quasar is always located at the position of the central galaxy in the halo. Simulations by Mihos & Hernquist (1996) show that during the merging of two disk galaxies of near-equal mass, gas inflows may occur at more than one stage during the encounter. After the initial collision, both galaxies form a strong central bar, and this drives an inflow of gas while the two galaxies are still widely separated. When the two galaxies finally merge, the remaining gas is again driven towards the centre of the remnant. The amount of gas channelled towards the centre during each event depends on the geometry of the encounter and on whether the galaxies have central bulges or not. These details of the fuelling process will affect the correlation functions on scales where tidal interactions between galaxies become important. Kochanek, Falco & Munoz (1999) have pointed out that if fuelling occurs during galaxy encounters, the amplitude of the quasar autocorrelation function on small scales would be enhanced over a simple power-law extrapolation from large radii. We do not address these issues in our simulations, but Fig. 5 illustrates what happens if we relax the assumption that quasars are always central objects and allow the quasar to be located at the position of a random galaxy in the halo. ξ_{QG} is now much shallower on scales smaller than $\sim 1\,h^{-1}$ Mpc.

It is useful to define the quantity $b_{QG}(R)$ as the ratio of the amplitude of the quasar/galaxy cross-correlation function $\xi_{QG}(R)$ to that of the galaxy autocorrelation function $\xi_{GG}(R)$:

$$b_{QG}(R) = \xi_{QG}(R)/\xi_{GG}(R). \quad (3)$$

Kauffmann, Nusser & Steinmetz (1997) have shown that when smoothed on scales larger than $\sim 1\,h^{-1}$ Mpc, the relation between the galaxy and dark matter density fields in *N*-body simulations is well described by a linear biasing relation for galaxies of all types and luminosities, so that $\delta_G = b_G \delta_{DM}$. Likewise, the quasar density field δ_Q may be written $\delta_Q = b_Q \delta_{DM}$. The quantity b_{QG} thus measures the ratio b_Q/b_G, i.e. the relative bias of quasars and galaxies.

The behaviour of b_{QG} as a function of radius is shown in Fig. 6 for galaxy samples selected in a variety of different ways. We see that on scales larger than $\sim 1\,h^{-1}$ Mpc, $b_{QG}(R)$ depends very little on the way in which galaxies are selected in the simulation. This is not surprising. As we have noted, in CDM cosmologies the clustering amplitude of present-day haloes is weakly dependent on

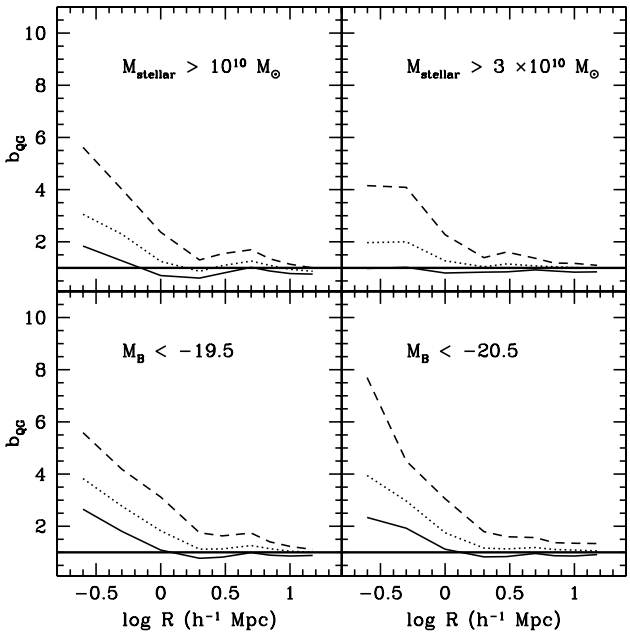

Figure 6. $b_{QG}(R)$ for galaxy samples selected in different ways in the simulation. Solid, dotted and dashed lines show results for quasars with $M_B = -22.5$, -23.5 and -24.5. Results are for our fiducial model with $t_q = 3 \times 10^7$ yr at a redshift $z = 0.4$.

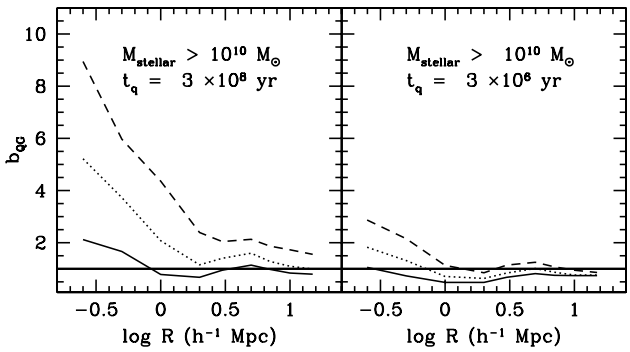

Figure 7. $b_{QG}(R)$ for long and short quasar lifetimes. Solid, dotted and dashed lines show results for quasars with $M_B = -22.5$, -23.5 and -24.5. Results are shown at $z = 0.4$.

mass for haloes less massive than $\sim 10^{13}\,M_\odot$. This corresponds to the characteristic mass (M_*) of non-linear objects at the present day. As discussed by Jing (1998), haloes smaller than this are almost unbiased tracers of the underlying dark matter distribution. On the other hand, the clustering amplitude is a strong function of mass for haloes more massive than M_*. Because low-redshift L_* galaxies are located primarily in haloes of $\sim 10^{12}\,M_\odot$ and quasars are found in haloes more massive than $10^{13}\,M_\odot$ for all values of t_q (Fig. 1), b_{QG} is a sensitive probe of mass distribution of the haloes hosting quasars, but not of the masses of the haloes that contain galaxies. In Fig. 6, brighter quasars appear more 'biased' than fainter quasars because they are located in more massive dark matter haloes. We note that the bias parameter will be considerably more sensitive to galaxy selection at high redshifts, where galaxies bright enough to be detected are located in haloes more massive than M_* at that epoch.

Fig. 7 demonstrates that $b_{QG}(R)$ is strongly dependent on the quasar lifetime t_q. For long lifetimes, there are large predicted differences in the clustering amplitudes of bright and faint quasars, particularly on scales between 1 and $2\,h^{-1}$ Mpc. For short lifetimes (10^6 yr), the differences between the clustering amplitudes of bright and faint quasars are small. Our fiducial model is intermediate between these two cases. Low redshift quasars with $M_B = -24.5$ are predicted to be clustered ~ 1.5 times more strongly than quasars with $M_B = -22.5$ on scales larger than $3\,h^{-1}$ Mpc. On scales $\sim 1\,h^{-1}$ Mpc, the difference is predicted to be closer to a factor of 3, but this will depend on the location of the quasar in the halo.

It has been suggested previously (La Franca et al. 1998; Haehnelt et al. 1998; Haiman & Hui 2001; Martini & Weinberg 2001) that the amplitude of the quasar autocorrelation function constrains the quasar lifetime. Both ξ_{QQ} and ξ_{QG} probe the masses of quasar host haloes. In practice, ξ_{QG} provides a stronger constraint at low redshifts where the number density of quasars is very low. As seen in Fig. 7, the main difference between models with short ($t_q \sim 10^6$ yr) and long ($t_q \sim 10^8$ yr) lifetimes lies in the clustering amplitude of the brightest ($M_B < -24$) quasars. Because of the steep dependence of the quasar luminosity function on magnitude, there are very few such objects at low redshifts in any flux-limited survey. For example, in the 2dF 10k QSO catalogue (Croom et al. 2001a), which covers an effective area of 290 deg^2 of the sky, there are 815 quasars with $0.3 < z < 0.57$, but only 108 quasars in this redshift range have B-band magnitudes brighter than -24. However, because the mean separation between galaxies and quasars is a factor of 10 smaller than the mean separation between the quasars themselves, it will still be possible to obtain a robust measurement of ξ_{QG} for these objects, particularly if photometric or spectroscopic redshifts are available for the galaxies in the sample.

4 QUASAR/GALAXY CORRELATIONS AT HIGHER REDSHIFT

Fig. 1 shows that quasars of given optical luminosity are located in lower mass haloes at higher redshifts in the KH model. There are two reasons for this: (1) galaxies are more gas-rich at high redshifts, so that M_{acc} in equation (1) is larger for a galaxy of given mass at high z, and (2) the quasar lifetime t_q is shorter at higher redshift. Both these assumptions were necessary in order to explain the strong observed increase in the space densities of bright quasars from the present day out to $z \sim 2$ (see KH for a more detailed discussion).

One consequence of these assumptions is that quasars of given optical luminosity are located in less massive host galaxies at high redshifts. These predictions appear to have been confirmed in two recent studies (Rix et al. 2001; Ridgway et al. 2001), although the results of Kukula et al. (2001) indicate that quasar hosts at $z \sim 2$ may be somewhat more massive than predicted by the KH model.

The evolution of $b_{QG}(R)$ to high redshift is shown in Fig. 8. Our prediction is that the relative bias between quasars and galaxies *decreases* at high redshift. On scales larger than $1\,h^{-1}$ Mpc, the predicted evolution of b_{QG} depends only weakly on galaxy selection. On scales less than $1\,h^{-1}$ Mpc, the predicted evolution of b_{QG} is very sensitive to how galaxies are selected. The bias decreases more strongly with redshift if galaxies are selected by stellar mass than if they are selected by rest-frame B-band magnitude. (Note that a galaxy of fixed B-band magnitude has a smaller stellar mass at high redshift, because optical mass-to-light ratios increase strongly with age.)

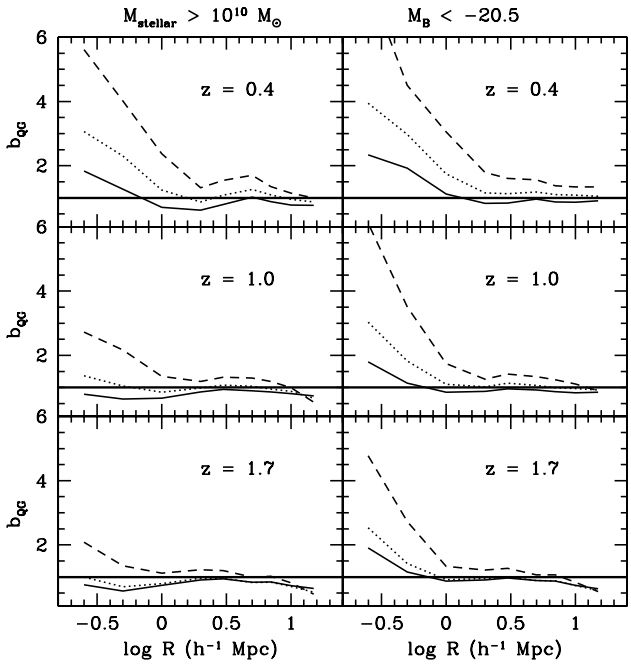

Figure 8. $b_{QG}(R)$ at $z = 0.4$, 1 and 1.7 for galaxies selected according to stellar mass and according to rest-frame B-band absolute magnitude. Solid, dotted and dashed lines show results for quasars with $M_B = -22.5$, -23.5 and -24.5. Results are shown for the fiducial model with $t_q(z = 0) = 3 \times 10^7$ yr.

5 EVOLUTION OF THE QUASAR AUTO-CORRELATION FUNCTION

We now turn to the predicted evolution of the quasar autocorrelation function ξ_{QQ}. On small scales, the number of quasar pairs will depend strongly on the physical processes responsible for channelling gas to the central black holes. However, on large scales, ξ_{QQ} simply probes the mass distribution of dark matter haloes in which quasars are located.

Our model predictions for the evolution of the clustering length R_0 as a function of redshift are shown in Fig. 9 for different choices of t_q (Note that quasar lifetimes are always quoted at z = 0). Results are shown for quasars with $-24 < M_B < -23$ (short-dashed lines) and for brighter quasars with $-26 < M_B < -25$ (long-dashed lines). Because the mean separation between quasars is more than 10 times the mean separation between galaxies, the quasar autocorrelations are always considerably more noisy than the quasar/galaxy cross-correlations. In Fig. 10, we plot the evolution of the comoving correlation length R_0 and compare it with recent measurements of the redshift-space clustering length s_0 from the 2dF QSO survey (Croom et al. 2001b). The sample analysed by Croom et al. (2001a) is flux-limited and is dominated by quasars with $M_B > -23$ at low redshifts and by quasars with $M_B < -26$ at $z > 2$. At redshifts $\sim$1, there are roughly equal numbers of galaxies in the two magnitude ranges $-24 < M_B < -23$ and $-26 < M_B < -25$. To facilitate comparison with the published results, we have also plotted the evolution of R_0 in our simulations adopting the same flux limits as in the 2dF data (solid lines). We only show results over the redshift range where the quasars in our simulation span the range of absolute magnitudes of the quasars in the data ($z = 0.6$–1.8).

We find that the data are in better agreement with short quasar lifetimes. It is reassuring that the same values of the lifetime

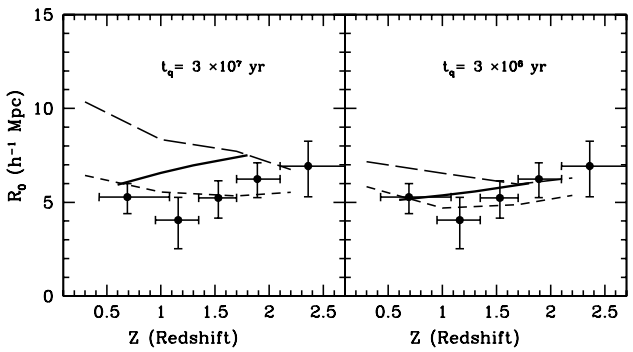

Figure 9. The evolution of the clustering length R_0 as a function of redshift for quasars with $M_B = -23.5$ (short-dashed lines) and $M_B = -25.5$ (long-dashed lines) for two different values of the quasar lifetime at $z = 0$. The data points are taken from Croom et al. (2001b). The solid line shows the evolution of R_0 for quasars with the same distribution of absolute magnitudes as in the data.

(10^6–10^7 yr) provide a good fit to the evolution of the quasar autocorrelation function and to the evolution of the quasar luminosity function (Fig. 2) at redshifts less than 1. Quasar lifetimes of 10^8 years are strongly disfavoured by the data.

6 SUMMARY AND DISCUSSION

We have studied the quasar/galaxy cross-correlation function ξ_{QG} and the quasar/quasar autocorrelation function ξ_{QQ} by embedding models for the formation and evolution of the two populations in cosmological N-body simulations. The galaxy evolution model has been described in detail by Kauffmann et al. (1999a). The quasar evolution model is that of Kauffmann & Haehnelt (2000) where supermassive black holes are formed and fuelled during major mergers. The correlation functions of quasars are interesting, because they probe physical processes operating on different scales.

On large scales ($>1\,h^{-1}$ Mpc), most of the contribution to ξ_{QG} and ξ_{QQ} comes from pairs in different dark matter haloes. We define a quasar/galaxy bias parameter b_{QG} as the ratio of the amplitude of ξ_{QG} to that of ξ_{GG}, the galaxy autocorrelation function. On scales larger than $1\,h^{-1}$ Mpc, b_{QG} depends very little on how galaxies are selected in the simulation. We obtain very similar results if we select galaxies according to stellar mass or according to optical luminosity.

On large scales, ξ_{QG} and ξ_{QQ} both probe the mass distribution of the dark matter haloes that contain quasars. If we adopt the assumptions of the KH model, they both provide a measure of the typical quasar lifetime. At low redshifts, ξ_{QG} provides a more efficient way of estimating the quasar lifetime than ξ_{QQ}, because an accurate measurement of ξ_{QG} is possible for a relatively small number of quasars. For the number of quasars available in current surveys, it will be possible to constrain the dependence of the lifetime on luminosity, on host galaxy type and on radio power. At redshifts greater than $\sim$1, where it becomes much more difficult to obtain spectroscopic redshifts for galaxies and where the space density of quasars is considerably higher, the quasar autocorrelation function ξ_{QQ} will probably prove more useful. We have used the simulations to calculate the evolution of ξ_{QQ}. Our models agree with the results of the 2dF QSO survey for quasar lifetimes in the range 10^6–10^7 yr.

On scales less than $1\,h^{-1}$ Mpc, ξ_{QG} and ξ_{QQ} are dominated by pairs within the same dark matter halo. The slope and amplitude of

ξ_{QG} on these scales depend not only on the number and the distribution of galaxies in the halo, but on the location of the quasar in the halo. In principle, it should be possible to constrain the density profiles of galaxies in dark matter haloes directly from the observations. When this is combined with the clustering amplitude of quasars measured on large scales, it should be possible to test whether quasars are located at the centres of dark matter potential wells, or whether they are more uniformly distributed throughout the halo. This would yield important information about the physical processes that were responsible for forming and fuelling the supermassive black holes found at the centres of galaxies today.

ACKNOWLEDGMENTS

We thank Brian Boyle and Scott Croom for helpful advice and for providing their data in machine readable format. This work was supported by the European Community Research and Training Network 'The Physics of the Intergalactic Medium'. GK thanks the Astrophysics Group of Imperial College for their hospitality.

REFERENCES

Bahcall J. N., Chokshi A., 1991, ApJ, 380, L9
Bahcall J. N., Schmidt M., Gunn J. E., 1969, ApJ, 157, L77
Boyle B. J., Shanks T., Croom S. M., Smith R. J., Miller L., Loaring N., Heymans C., 2000, MNRAS, 317, 1014
Brown M. J. I., Boyle B. J., Webster R. L., 2001, AJ, 122, 26
Croom S. M., Smith R. J., Boyle B. J., Shanks T., Loaring N. S., Miller L., Lewis I. J., 2001a, MNRAS, 322, L29
Croom S. M., Shanks T., Boyle B. J., Smith R. J., Miller L., Loaring N. S., Hoyle F., 2001b, MNRAS, 325, 483
Diaferio A., Kauffmann G., Balogh M. L., White S. D. M., Schade D., Ellingson E., 2001, MNRAS, 323, 999
Ellingson E., Green R. F., Yee H. K. C., 1991, ApJ, 371, 49
Finn R. A., Impey C. D., Hooper E. J., 2001, ApJ, 557, 578
Fisher K. B., Bahcall J. N., Kirhakos S., Schneider D. P., 1996, ApJ, 468, 469
Haehnelt M. G., Kauffmann G., 2000, MNRAS, 318, L35
Haehnelt M. G., Rees M. J., 1993, MNRAS, 263, 168
Haehnelt M. G., Natarajan P., Rees M. J., 1998, MNRAS, 300, 817
Haiman Z., Hui L., 2001, ApJ, 547, 27
Hartwick F. D. A., Schade D., 1990, ARA&A, 28, 437
Jing Y., 1998, ApJ, 503, 9
Kauffmann G., Haehnelt M., 2000, MNRAS, 311, 576
Kauffmann G., White S. D. M., 1993, MNRAS, 261, 921
Kauffmann G., Nusser A., Steinmetz M., 1997, MNRAS, 323, 999
Kauffmann G., Colberg J., Diaferio A., White S. D. M., 1999a, MNRAS, 303, 188
Kauffmann G., Colberg J., Diaferio A., White S. D. M., 1999b, MNRAS, 307, 529
Kochanek C. S., Falco E. E., Munoz J. A., 1999, ApJ, 510, 590
Kukula M. J., Dunlop J. S., McLure R. J., Miller L., Percival W. J., Baum S. A., O'Dea C. P., 2001, MNRAS, 326, 1533
La Franca F., Andreani P., Cristiani S., 1998, ApJ, 497, 529
McLure R. J., Dunlop J. S., 2001, MNRAS, 321, 515
McLure R. J., Kukula M. J., Dunlop J. S., Baum S. A., O'Dea C. P., Hughes D. H., 1999, MNRAS, 308, 377
Martini P., Weinberg D. H., 2001, ApJ, 547, 12
Mihos J. C., Hernquist L., 1996, ApJ, 464, 641
Mo H. J., White S. D. M., 1996, MNRAS, 282, 347
Ridgway S. E., Heckman T. M., Calzetti D., Lehnert M., 2001, ApJ, 550, 122
Rix H.-W., Falco E., Impey C., Kochanek C., Lehar J., McLeod B. A., Munoz J., Peng C., 2001, in Brainerd T., Kochanek C. S., eds, ASP Conf. Ser. Vol. 237, Gravitational Lensing. Astron. Soc. Pac., San Francisco, p. 169
Sheth R. K., Mo H. J., Tormen G., 2001, MNRAS, 323, 1
Springel V., White S. D. M., Tormen G., Kauffmann G., 2001, MNRAS, 328, 726
Wold M., Lacy M., Lilje P. B., Serjeant S., 2001, MNRAS, 323, 231
York D. G. et al., 2000, AJ, 120, 1579
Yee H. K. C., Green R. F., 1984, ApJ, 280, 79
Yee H. K. C., Green R. F., 1987, ApJ, 319, 28

This paper has been typeset from a TEX/LATEX file prepared by the author.